DYNAMIC PROPERTIES OF ALUMINIUM ALLOYS USED IN AUTOMOTIVE INDUSTRY

Wojciech Moćko

Motor Transport Institute
Centre for Material Testing
Jagiellońska Street 80, 03-301 Warsaw, Poland
tel.: +48 22 43-85-400, fax: +48 43-85-401
e-mail: wojciech.mocko@its.waw.pl

Zbigniew L. Kowalewski

Institute of Fundamental Technological Research
Polish Academy of Sciences
Pawińskiego Street 5B, 02-106 Warsaw
tel.: +48 22 8261281, fax: +48 22 8269815
e-mail: zkowalew@ippt.gov.pl

Abstract

Around 20% of CO2 emitted as a result of human activity on Earth comes from transportation. One of the ideas, which lead to diminishing of the greenhouse gases emission, is reducing of fuel consumption. It may be achieved by introducing a new powertrain solutions as well as lowering overall vehicle weight. The reduction of vehicle weight may be obtained by both a new design of part and structures and application of a new materials i.e. aluminium alloys. It has to be emphasised that weight reduction is very important for combustion engine driven vehicles and electric driven vehicles as well. Mass lowering is especially desirable in the case of electric vehicles because they typically have a very narrow operational range usually lower than 200 km. Therefore even small weight reduction decreases energy consumption of EV and as a consequence increases its range, which is a crucial parameter for users.

The results presented in this article were focused on high strength aluminium alloys of 6082-T6 and 7075-T6 types. Applying of those materials enables mass lowering of structures up to 50%, maintaining original functionality. Moreover, aluminium alloys may be also used in energy absorbing structures. The goal of tests was to obtain data required in FE analysis. In order to simulate dynamic phenomenon i.e. vehicle crash investigation of the stress-strain curves of alloys were carried out at wide range of strain rates using Hopkinson bar

Keywords: *road transport, simulation, combustion engines, air pollution, environmental protection*

1. Introduction

Currently, the passenger protection during collision impact is the one of most significant problems from those taken into account during vehicle design process [1]. In typical solutions, the vehicle structure is divided into two basic parts [2]:

– crumple zones that absorb the impact energy,
– a rigid passenger compartment.

Due to more and more strict requirements for vehicle safety and comfort, the size of various vehicle elements increases, leading to higher total mass of vehicle. As it follows from the analysis performed for passenger cars belonging to the „C" segment [3], the average mass of a vehicle has increased from 800 kg to 1200 kg in 1982 – 2002. In case of electric vehicles, this problem is even more noticeable, since installing of traction batteries results in further increase of vehicle mass by another 200 to 300 kg [4].

In case of vehicles driven by an electric motor, reduction of vehicle mass is one of the ways to increase the range of the vehicle. It should be emphasized that today the short range (of about 150 km) is the basic factor that limits the development of electric vehicle market. For vehicles driven by combustion engines reduction of vehicle mass allows for reducing the consumption of fuel and, consequently, the ownership costs and the amount of carbon dioxide emitted to the atmosphere. It is estimated that reduction of vehicle mass by 100 kg reduces fuel consumption by about 0.35 l, and this amount corresponds to reduction of CO2 emission by 9 g/km [3]. The reduction of vehicle mass also brings additional benefits such as better acceleration, better braking efficiency, better handling and higher comfort.

Use of aluminium alloys for construction of vehicles is one of methods for reducing the vehicle mass, since the density of aluminium alloys amounts to 2700 kg/m3 – one third of the one for steel (7600 kg/m3). To ensure mechanical properties comparable with those for steel, it is necessary to use aluminium elements with cross sectional areas larger than for steel elements. Therefore, the average mass reduction is slightly smaller than the reduction resulting from just comparing the specific gravity values for both materials. The effective mass reduction of the element made of aluminium alloy as compared with the steel one amounts to about 50%. The direct reduction of vehicle mass causes the so-called "secondary" mass reduction, being the effect of smaller dimensions and sizes necessary for other structural elements of vehicle. The aluminium content in vehicle structures increases as the new alloys and design solutions are developed. The mass of aluminium alloys used in the vehicle has increased from 40 kg in 1980 to approximately 130 kg in 2005 [3]. As it follows from the detailed study of vehicle market in China [5], the emission of dangerous substances will be clearly reduced when the aluminium content will increase above 330 kg.

The alloys of 5000 and 6000 series [6], which allow constructing of virtually entire structure of vehicle body, are of particular interest in automotive sector. Using the 6060-T6 alloy, the space frame-based design of vehicle was developed which has fulfilled the Federal Motor Vehicle Safety Standards' requirements for frontal impact test.

Aluminium is a good material for construction of energy-absorbing elements. For aluminium, the value of parameter describing the mass-specific energy absorption capacity is twice of that for mild steels and comparable with the latest high-strength steels (HSS steels). The behaviour of a given element during impact depends on [7]: shape, wall thickness or use of filling material [8].

The materials used for vehicle structures must show the following, often mutually opposing, features:

– ease for plastic forming,
– high strength,
– good plasticity,
– low mass,
– low production costs,
– joining easiness.

Therefore, for individual functional elements of a vehicle various materials with properties and parameters suitable for a given element are used (e.g. steels, aluminium alloys, magnesium alloys and fibre reinforced plastic composites).

With the increasing interest in electric vehicles, the design guidelines change because safety of vehicle with large mass of traction batteries must be ensured as well and because the potential applications of electric vehicles are slightly different that for conventional ones. In UE countries some projects are recently carried out concerning design and mass reduction of vehicles with electric motors and combustion engines (e.g. ELVA, MyCar, Green City Car, and ALIVE), or concerning use of smart materials for noise reduction (e.g. InMAR).

The goal of this study was to obtain mechanical properties of 6082-T6 and 7075-T6 aluminium alloys, which can be applied in constitutive modelling and further used in Finite Element simulation.

Aluminium alloy 6082 is a medium strength alloy with excellent corrosion resistance. It has the highest strength of the 6xxx series. T6 tempered aluminium alloy 6082 shows excellent performance in machining operations. This grade substitutes to the conventional 6061 alloy in many structural applications in which improved mechanical properties are required. It is widely used in transport and structural applications in which high stress resistance is essential. The chemical composition of the material (% of weight) is reported in Tab. 1. The major alloying elements are silicon (1.00 wt. %), magnesium (0.78 wt. %) and manganese (0.50 wt. %).

Aluminium alloy 7075 is a high strength alloy that displays moderate strength/toughness relationships. It has been the reference grade of the 7xxx series for the aeronautical industry since its development. T6 tempered aluminium alloy 7075 shows excellent stress and strain resistance properties. Aluminium alloy 7075-T6 is used extensively in the aircraft and aerospace industries for highly stressed structural parts. The chemical composition of the material (% of weight) is reported in Tab. 1. The major alloying elements are zinc (5.73 wt. %), magnesium (2.42 wt. %) and copper (1.52 wt. %).

Tab. 1. The chemical composition of the tested aluminium alloy (wt. %)

Alloy	Si	Fe	Cu	Mn	Mg	Zn	Ti	Cr	Pb
6082-T6	1.00	0.32	0.07	0.50	0.78	0.05	0.04	0.03	0.02
7075-T6	0.09	0.22	1.52	0.12	2.42	5.72	0.06	0.19	0.02

The specimens had the following dimensions:

- diameter φS0=10mm and thickness tS0=5mm in the case of low rate and high rate compression tests,
- diameter φS0 = 1.5 mm and thickness tS0 = 0.5 mm in the case of very high strain rate experiments.

The samples used in all of the tests performed were machined from extruded round bars of 15mm diameter using the electro-discharging machine (EDM). The tested loading path is the one corresponding to the longitudinal direction of the extruded bars. Interfaces were lubricated using MoS_2 in order to reduce friction effects between the anvil and specimen under compression.

2. Experimental methods

Low rate compression tests were conducted using a servo-hydraulic testing machine at room temperature within the range of strain rates $4 \cdot 10^{-4}\ s^{-1} < \dot{\varepsilon} < 10^{-1}\ s^{-1}$. An electro-mechanical extensometer was applied for the axial strain measurements.

High rate compression experiments with strain rates in the range of were carried out using a conventional SPHB arrangement [8]. The test stand, presented in Fig. 1, was equipped with incident (8) and transmitter (9) bars 20 mm in diameter and 1000 mm in length, which were made of high strength maraging steel, σy = 2100 MPa. The signals acquired from the strain gauges (7) were amplified by the wideband bridge circuit (3) and digitised by an oscilloscope (4). The initial velocity of the striker (5), which was accelerated in a pressure gas launcher (1) was measured by two sets of diodes and photodetectors coupled to a digital counter (2).

The stress σ(t,) strain ε(t) and strain rate $\dot{\varepsilon}(t)$ in the specimen were calculated using the following equations:

$$\sigma(t) = E\left(\frac{A}{A_S}\right)\varepsilon_T(t), \tag{1}$$

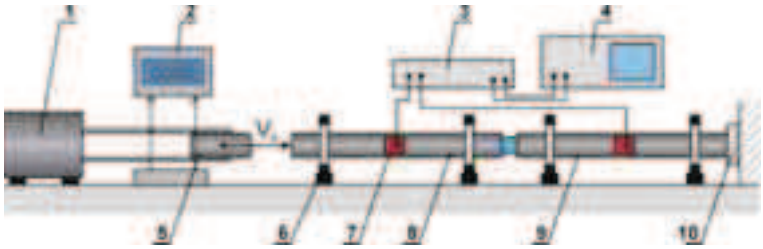

Fig. 1. Schematic representation of the SHPB arrangement. (1) pneumatic gun; (2) striker velocity measurement; (3) strain gauges bridge and amplifier; (4) digital recorder; (5) striker bar; (6) support; (7) strain gauge; (8) incident bar; (9) transmitter bar; (10) damper

$$\varepsilon(t) = -\frac{2C_0}{L}\int \varepsilon_R(t)dt\,, \tag{2}$$

$$\dot{\varepsilon}(t) = \frac{d\varepsilon(t)}{dt} = \frac{-2C_0}{L}\varepsilon_R(t)\,, \tag{3}$$

where

$\varepsilon_T(t)$ – transmitted wave,
$\varepsilon_R(t)$ – reflected wave,
A, A_S – transversal cross-section of the bar and specimen respectively,
L – specimen length,
E – Young's modulus of the bar material,
C_0 – velocity of the elastic wave in the bar.

Very high rate compression experiments with strain rates in the range of were carried out using a MDICT arrangement developed at the Institute of Fundamental Technological Research in Warsaw [9]. The test stand shown in Fig. 2 was equipped with a small transmitter bar (3) of 3 mm diameter and 248 mm length, which was made of high strength maraging steel, σ_y = 2100 MPa. Miniature strain gauges (4) were bonded symmetrically on both sides of the bar, 22 mm from the edge on which the specimen was placed. The strain gauges were connected in series to eliminate potential bending effect disturbances of their measurements. The strain gauge bridge measuring system has a wide transmission band to ensure the correct operation of very short (lasting a dozen or so μs) signals. The bar was placed inside a decelerator tube (5), which was mounted in supports with a variable separation (7) slightly ahead of the Hopkinson bar (3). Both the tube and the bar were attached to the bumper (8) to absorb the mechanical wave propagated along the bar. The tube could be exactly adjusted to the axis of the striker (2) by a support (6), which prevented vibrations. The projectile was made of high strength maraging steel, σ_y = 2100 MPa, with the following dimensions: 11 mm diameter and 12.5 mm length. For this arrangement, the pneumatic launcher (1) allowed impact velocities up to 150 m/s. The launcher tube (1) was 840mm in length. The striker (2) had a diameter slightly larger than the inner diameter of the decelerator tube (5); thus, the impactor triggered controlled deformation of the specimen until it the striker was stopped by the tube. The relative distance between the tube and the transmitter bar could be varied from 0 to 2.0 mm. This distance defined the maximum deformation of the specimen.

The stress σ(t,) strain ε(t) and strain rate $\dot{\varepsilon}(t)$ in the specimen were calculated using the following equations:

$$\sigma(t) = E\left(\frac{A}{A_S}\right)\varepsilon_T(t)\,, \tag{4}$$

$$\varepsilon(t) = \frac{1}{L}\left[U_A(t) - C_0\int \varepsilon_T(t)dt\right], \tag{5}$$

$$\dot{\varepsilon}(t) = \frac{1}{L}\left[\frac{dU_A(t)}{dt} - C_0\,\varepsilon_T(t)\right], \tag{6}$$

where UA(t) – striker/specimen interface displacement.

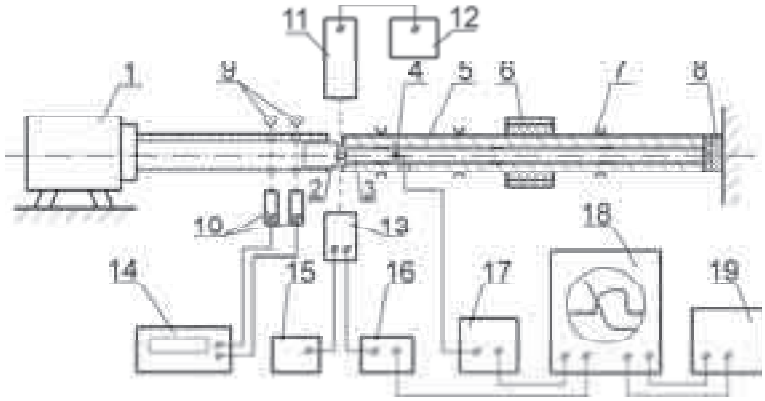

Fig. 2. Schematic representation of the MDICT arrangement. (1) pneumatic gun; (2) striker; (3) transmitter bar; (4) strain gauges; (5) decelerator tube; (6) main support; (7) supports; (8) damper; (9) light sources; (10) photodiodes; (11) laser diode; (12) supply unit of 11; (13) photodiode (displacement measurement); (14) time counter; (15) supply unit of 13; (16) DC amplifier; (17) strain gauges amplifier; (18) digital oscilloscope; (19) data acquisition system

3. Results

Figure 3 shows results of static compression tests of 6082-T6 and 7075-T6 aluminium alloys within the range from $4x10^{-4}s^{-1}$ to $1x10^{-1}s^{-1}$. Both materials shows very narrow effects of work hardening which may be observed only at low strains below ε=0.1. Moreover, influence of the deformation rate on the flow stress is negligible.

The stress-strain curves, obtained using SHPB method within the range from $1.1x10^{3}s^{-1}$ to $5.3x10^{3}s^{-1}$ are presented in Fig. 4. The typical oscillations caused by dispersion of an elastic wave in the Hopkinson bar may be observed, however they does not influence the results. Work hardening effect in the case of SHPB tests is comparable to those obtained at the static deformation rates. The difference in comparison to the low rate experiments is presence of strain rate hardening effects. It may be observed as an increase of the flow stress magnitude with increase of a strain rate.

The results of the MDICT tests within the range from $5x10^{4}s^{-1}$ to $1.1x10^{5}s^{-1}$ are presented in Fig. 5. Part of the curves below strain equal to 0.1 is excluded from analysis because at the beginning of the test force equilibrium condition is not satisfied. More information concerning application of MDICT may be found in previous works [10-13]. It may be observed that flow stress at very high strain rates increases sharply in comparison to the low or high rates (SHPB). This phenomenon is related to the presence of viscous-drag component in the overall flow stress [14]. The viscous-drag component usually occurs at rates higher than $5x10^{3}s^{-1}$.

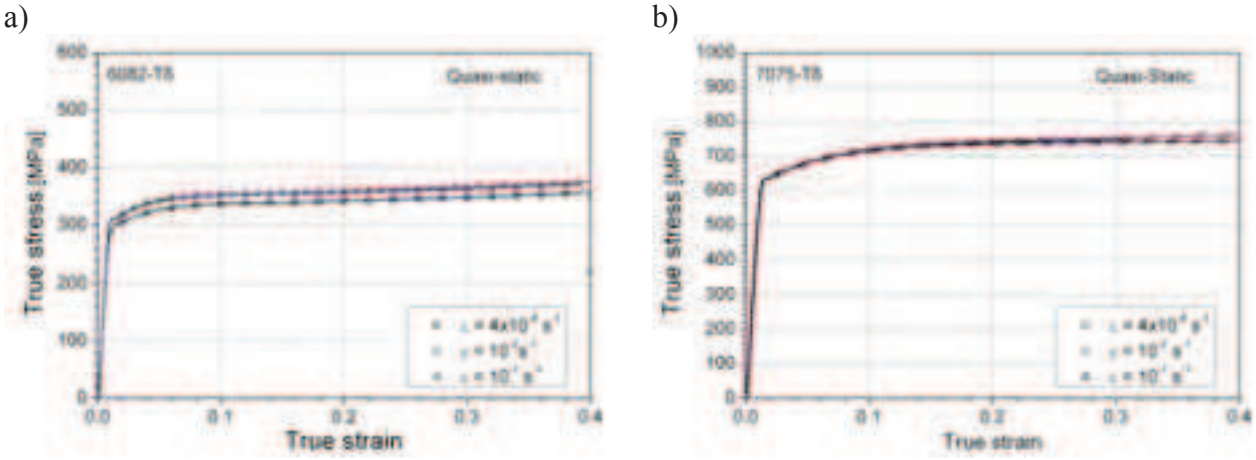

Fig. 3. Static compression tests; a) AA 6082-T6; b) AA 7075-T6

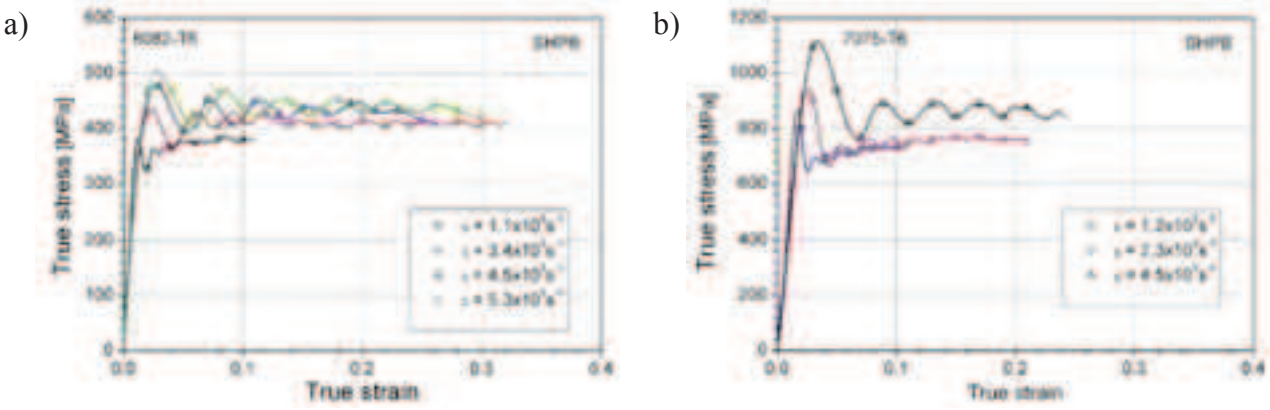

Fig. 4. Split Hopkinson pressure bar tests; a) AA 6082-T6; b) AA 7075-T6

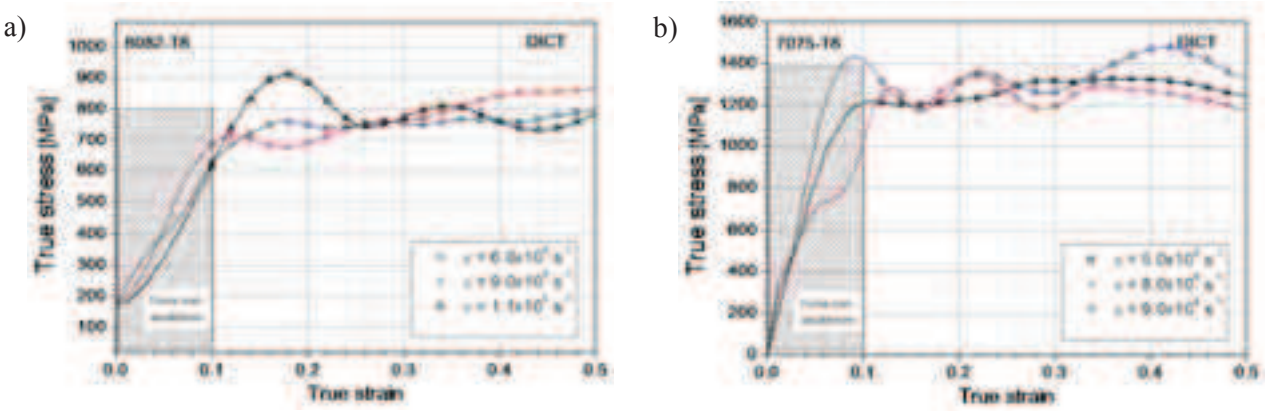

Fig. 5. Miniaturised direct impact compression tests; a) AA 6082-T6; b) AA 7075-T6

Figure 6 shows strain rate sensitivity dependence for both tested alloys. Moreover, particular experimental method is marked on the chart. It can be seen that aluminium alloys doesn't shows any hardening effects for strain rates lower than $1x10^3s^{-1}$. However, above this limit sharp increase of the flow stress may be observed. As it was mentioned before, this property is related to viscous-drag component presence. The intensity of strain rate hardening phenomena is comparable for both materials.

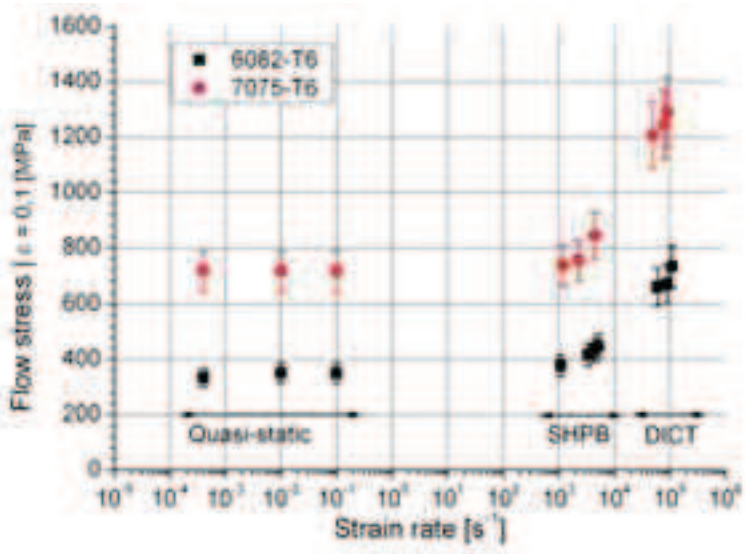

Fig. 6. Strain rate sensitivity of AA 6082-T6 and AA 7075-T6

4. Summary

The compressive stress strain curves of the 6082-T6 and 7075-T6 aluminium alloys were determined at strain rates within the range from $4x10^{-4}s^{-1}$ to $1.1x10^{5}s^{-1}$. Tests were carried out at room temperature using various methodologies. The obtained results may be used for the purposes of FEM modelling, especially when dynamic experiments are simulated i.e. vehicle crash, explosions or ballistic impacts.

Acknowledgements

This work was partially supported by the Polish National Centre for Research and Development (Project No. NR10-0020-10).

References

[1] Witteman, W. J., *Improved Vehicle Crashworthiness Design by Control of the Energy Absorption for Different Collision Situations*, Doctoral dissertation, Technische Universiteit Eindhoven, 1999.
[2] Paul, D. B., *Vehicle crashworthiness and occupant protection, edited by Priya Prasad, Jamel E. Belwafa*, American Iron and Steel Institute, Southfield, Michigan 2004.
[3] *Aluminium in Cars*, European Aluminium Association, 2007.
[4] Moćko, W., Wojciechowski, A., Ornowski, M., *Perspektywy rozwoju rynku samochodów elektrycznych w najbliższych latach,* Transport Samochodowy, 1/2011, pp. 63-71, 2011.
[5] Du, J. D., Han, W. J., Peng, Y. H., Gu, C. C., *Potential for reducing GHG emissions and energy consumption from implementing the aluminum intensive vehicle fleet in China*, Energy, Vol. 35, pp. 4671-4678, 2010.
[6] Miller, W. S.,*Recent development in aluminium alloys for the automotive industry*, Materials Science and Engineering, Vol. A280, pp. 37-49, 2000.
[7] Bouchet, J., Jacquelin, E., Hamelin, P., *Static and dynamic behavior of combined composite aluminium tube for automotive applications,* Composites Science and Technology, Vol. 60, pp. 1891-190, 2000.
[8] Lindholm, U. S., *Some experiments with the split hopkinson pressure bar*, J. Mech. Phys. Solids*,* Vol. 12, pp. 317-335, 1964.
[9] Malinowski, J. Z., Klepaczko, J. R., Kowalewski, Z. L., *Miniaturized Compression Test at Very High Strain Rates by Direct Impact*, Exp. Mech., Vol. 47, pp. 451-463, 2007.
[10] Moćko, W., Kowalewski, Z. L., *Opracowanie i weryfikacja modelu MES zminiaturyzowanego stanowiska do badań metodą bezpośredniego uderzenia pocisku w próbkę*, Transport Samochodowy, Vol. 32, pp. 97-105, 2011.
[11] Moćko, W., Kowalewski, Z. L., *Dynamic Compression Tests – Current Achievements and Future Development*, Engineering Transactions, Vol. 59, pp. 1-14, 2011.
[12] Moćko, W., Kowalewski, Z. L., *Numerical modelling of the miniaturized direct impact compression test method*, Proccedings of th 28th Danubia-Adria-Symposium on Advances in Experimental Mechanics, Scientific Society for Mechanical Engineering, pp. 119-120, Hungary 2011
[13] Moćko, W., Rodríguez-Martínez, J. A., Kowalewski, Z. L., Rusinek, A., *Compressive viscoplastic response of 6082-T6 and 7075-T6 aluminium alloys under wide range of strain rate at room temperature: Experiments and modelling*, Strain, Accepted for publication.
[14] Rusinek, A., Rodriguez-Martinez, J. A., Klepaczko, J. R., Pęcherski, R. B., *Analysis of thermo-visco-plastic behaviour of six high strength steels*, Mater. Des., Vol. 30, pp. 1748-1761, 2009.